Quantitative phase evaluation of dynamic changes on cell membrane during laser microsurgery

Lingfeng Yu,[*,†] Samarendra Mohanty,[†] Gangjun Liu, Suzanne Genc, Zhongping Chen,[*] and Michael W. Berns
University of California, Irvine, Beckman Laser Institute, Irvine, California 92612

Abstract. The ability to inject exogenous material as well as to alter subcellular structures in a minimally invasive manner using a laser microbeam has been useful for cell biologists to study the structure-function relationship in complex biological systems. We describe a quantitative phase laser microsurgery system, which takes advantage of the combination of laser microirradiation and short-coherence interference microscopy. Using this method, quantitative phase images and the dynamic changes of phase during the process of laser microsurgery of red blood cells (RBCs) can be evaluated in real time. This system would enable absolute quantitation of localized alteration/damage to transparent phase objects, such as the cell membrane or intracellular structures, being exposed to the laser microbeam. Such quantitation was not possible using conventional phase-contrast microscopy.
© *2008 Society of Photo-Optical Instrumentation Engineers.*
[DOI: 10.1117/1.2997375]

Keywords: laser scissors; short-coherence interference microscopy; quantitative phase imaging; optical micromanipulation; cellular damage.

Paper 08175LR received Jun. 6, 2008; revised manuscript received Aug. 19, 2008; accepted for publication Aug. 22, 2008; published online Oct. 21, 2008.

Since the appearance of the laser in the 1960s as a source of powerful and highly focused light, researchers have been using lasers in the life sciences and in medicine. The laser microbeam, also termed "laser scissors," uses lasers to alter and/or to ablate intracellular organelles and cellular and tissue samples and, today, has become an important tool for cell biologists to study the molecular mechanism of complex biological systems by removing individual cells or subcellular organelles.[1] Laser scissors were used to study cell structure and function by ablation of chromosomes, mitotic organelles, mitochondria, or other subcellular structures.[2] Single cells or groups of cells have been perforated for injection of exogenous materials[3,4] and have even been cut open by laser scissors to free the internal constituents for analysis[5] and to study the developmental fate of those cells in developing organisms—such as in the formation of the nervous system.[6] Clinically, laser scissors have also been used to reduce the thickness of the zona pellucida layer of the ovum in order to improve human *in vitro* fertilization.[7]

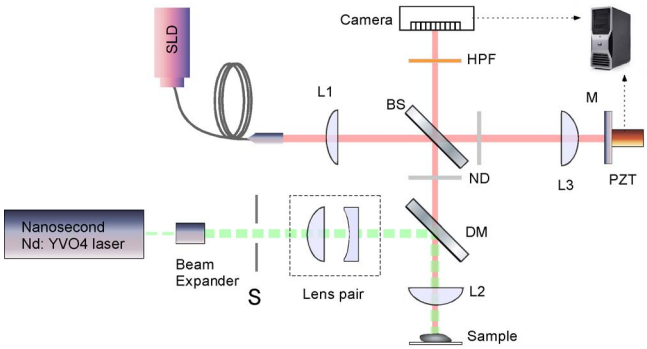

Fig. 1 Schematic of the experimental setup. The Ls are various lenses; BS is a beamsplitter; DM is a dichroic mirror reflecting IR and transmitting the green nanosecond laser; NDs are neutral density filters; HPF is a high-pass filter for IR light; S is a shutter; and M is a mirror.

However, visualization of transparent microscopic biological specimens (such as living cells and their intracellular constituents) being manipulated by a laser microbeam is difficult using conventional bright-field microscopy. Although Zernike phase-contrast microscopy[8] and Nomarski differential interference contrast (DIC) microscopy[9] are the most widely used in laser microsurgery systems, quantitative phase imaging is not feasible with these techniques. Also, there are significant artifacts in the images, such as a halo in phase-contrast microscopy and the disappearance of contrast along the direction perpendicular to the shear in DIC microscopy.

Quantitative phase imaging[10–14] is important because it allows the determination of the optical thickness profile of a transparent object with sub-wavelength accuracy. We report for the first time a quantitative phase laser microsurgery (QPLM) system, which takes advantage of the combination of laser scissors and short-coherence interference microscopy.[15] Quantitative phase images are recorded during the process of laser microsurgery on red blood cells (RBCs), and thus, dynamic changes in phase can be continuously evaluated. The introduction of quantitative phase imaging in laser microbeams will make it possible to evaluate quantitatively the damage or the repair of the cell or cell organelle in real time. For example, this system would enable monitoring of processes such as optoporation where the cell membrane is transiently altered by the use of laser scissors.

The design of the quantitative phase laser microsurgery system is described in Fig. 1. After passing through a 5× beam expander, the second-harmonic 532-nm green scissors beam from a nanosecond Nd: YVO_4 laser (20 KHz, 12 ns, Coherent, Inc.. Santa Clara, California) is guided through a shutter and a lens pair, deviated by a dichroic mirror (DM) and focused onto a small spot of the sample by a (20×) objective, L2. The lens pair, composed of a concave and a convex lens, is introduced to match the focal plane with the imaging plane of the objective. For the purpose of quantitative phase imaging, the infrared (IR) light from a superluminescent diode (SLD; BWC-SLD, B&W TEK) of 1.3-μm center wavelength and ~8-μm coherence length is focused by a lens, L1, and split into a Linnik-based interferometer, which uses two identical objectives (L3 and L2) in both the reference and the sample arms to match the wavefronts and to

[†]These authors contributed equally to this work.
*Tel: 9498248975; E-mail: yulingfeng@gmail.com; z2chen@uci.edu

1083-3668/2008/13(5)/050508/3/$25.00 © 2008 SPIE

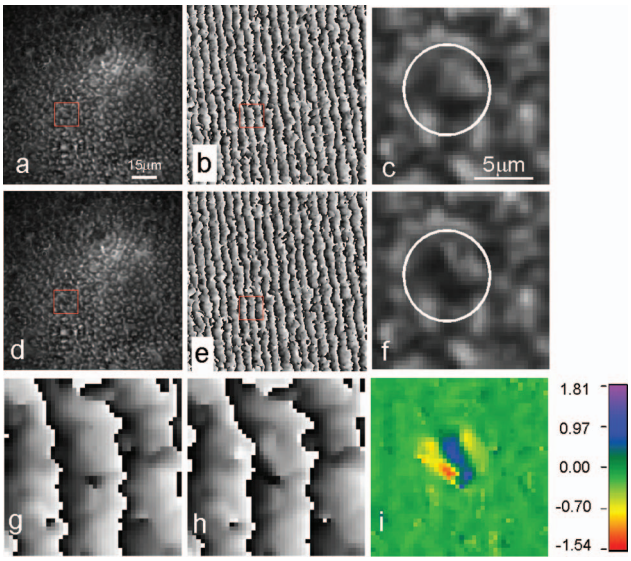

Fig. 2 Quantitative phase images of RBCs. (a) Bright-field image, (b) interference phase map, and (c) enlarged bright-field image before laser microsurgery. Similarly, (d)–(f) are those for after laser microsurgery. Figures (g) and (h) show the enlarged phase maps of (b) and (e), respectively. Figure (i) shows the phase variation after laser microsurgery. Images in (a) and (b) and (d) and (e) are the same magnification. Images in (c) and (f) to (i) are for the same selected area and have the same magnification.

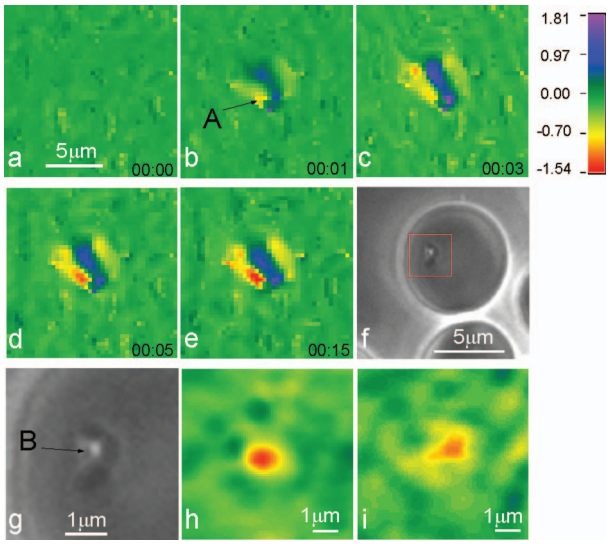

Fig. 3 Time-lapse (in seconds) images showing dynamic changes of phase variation during laser microsurgery of RBCs. (a) Before microirradiation and after (b) 1 s, (c) 3 s, (d) 5 s, and (e) 15 s of irradiation. (f) Phase contrast image of a microdissected RBC (note the phase changes in the surrounding area) in high magnification (63 ×/1.4 NA). (g) Magnified image of the selected area in (f). (h) Symmetric laser-induced phase variation (lesion) by a well-focused laser beam and (i) asymmetric phase variation (lesion), by a slightly defocused laser beam through a 40×/0.65 NA objective.

compensate for chromatic and other optical aberrations. All of the reflections from the object or the reference mirror are directed toward an InGaAs camera (SU1024-1.7T, Sensors Unlimited) through the imaging objective lens, L2. The camera has an array of 640×512 pixels with a 25-μm pitch size and 12-bit grayscale output with an acquisition speed of 109 frames per second. The reference mirror is positioned at an equal distance with respect to the object focal plane within the coherence length of the SLD and dithered by a piezotransducer (E-662, Physik Instrumente) to acquire four consecutive frames of $\pi/2$ phase shifts. Both the amplitude and the phase images are then calculated by phase-shifting interferometry.[15]

In order to demonstrate the effectiveness of this method, RBCs harvested from a healthy volunteer were smeared onto a glass coverslip and brought into focus by adjusting a three-axis translation stage in the QPLM system. The lens pair was then used to fine-adjust the focal plane of the laser microbeam onto the sample. The shutter of the laser microbeam system remained off during the alignment process. Figure 2(a) shows a bright-field image of the RBCs before laser microirradiation. A custom-designed program was used to observe the sample phase map in real time and could be triggered to record automatically all of the phase maps of the RBC sample after and during the opening of the shutter. Figure 2(b) shows the phase map just before the shutter of the microbeam was opened, and Fig. 2(c) shows the enlarged bright-field image of a selected area (red window) in Fig. 2(a). Similarly, Figs. 2(d)–2(f) show the bright-field images and phase maps about 5 s after the shutter opening. With a pulse frequency of 20 kHz, the average power of the laser microbeam coming out of the 20×/0.35 NA objective was measured to be 4 mW, which corresponds to 0.2 μJ/pulse. With a spot size of 2 μm and a pulse width of 12 ns, this corresponds to a peak irradiance of 5×10^8 W/cm^2. The enlarged phase maps before and after laser irradiation are shown in Figs. 2(g) and 2(h). The dynamic phase change of the sample [Fig. 2(i)] was traced by calculating the unwrapped phase difference between the two maps above. Subsequent to a laser-induced lesion, a very subtle change in the bright-field images of the cells [see circled region in Figs. 2(c) and 2(f)] was observed. However, by tracking the phase changes, QPLM makes it possible to evaluate quantitatively the dynamic changes in the cell membrane during laser microsurgery.

Figure 3 shows an example of several time-lapse images of the RBC phase change due to different laser microbeam exposure times. From the quantitative phase information, the change in physical thickness of cells can be estimated using the equation $\Delta d=\lambda(\Delta\varphi/4\pi)/(n-n_0)$, where λ is the wavelength (1.3 μm) of the SLD source, $\Delta\varphi$ is the phase change, and $(n-n_0)$ is the index difference between the cells and the surrounding buffer ($n_0=1.33$). For the illumination wavelength of 1.3 μm, we assume the RBCs to be characterized by a constant refractive index $n_c=1.41$ at room temperature.[16,17] As shown in Fig. 3(b), the phase change at the focused spot A of a single RBC is about −0.7 radians, which corresponds to a −0.905 μm overall height change of the cell. Figures 3(d) and 3(e) show the effect of long-term (15 s) laser microirradiation. As can be seen in the figures, no significant increase in phase change is observed as the laser exposure is increased from 5 to 15 s. This demonstrates precise photothermal confinement of the nanosecond laser microbeam employed in this system, since the pulse is much less than the theoretically calculated thermal diffusion time of 2 μs. While for short exposures of laser microbeam irradiation, sealing of the membrane is expected, no sealing was observed for major cuts

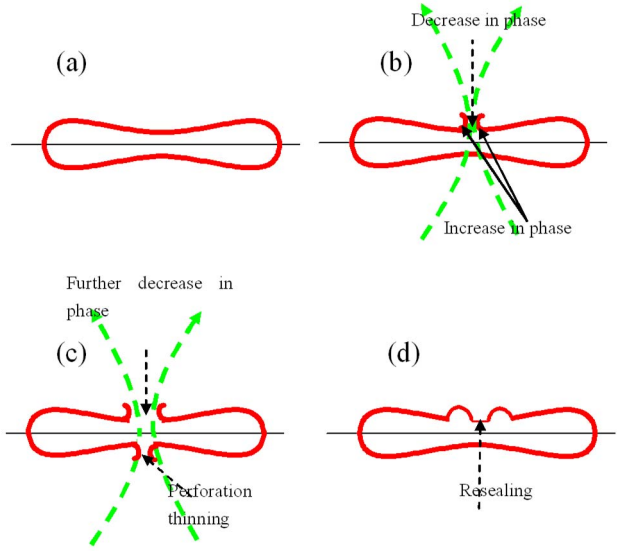

Fig. 4 Schematic explanation of the phase change observed in microirradiated and collateral regions of the RBC. (a) Cross-sectional view of unirradiated RBC; (b) membrane damage at the microirradiated spot and buckled collateral positions; (c) increase in membrane damage along the axial direction with an increase in laser dose; and (d) resealing of membrane after switching off the laser microbeam.

induced after long exposures. For comparison, we show in Figs. 3(f) and 3(g), the phase contrast images of a laser-microdissected (using 63×/1.4 NA phase objective) RBC for a short exposure time similar to Fig. 3(b). The phase change (bright) was observed in the focused spot B surrounded by dark regions, which indicates buckling of the RBC membrane. A similar effect can be noticed and quantitated in Fig. 3(b). For long exposures, we found an elongated phase change [Figs. 3(c)–3(e)]. This can be attributed to the relative movement of the sample with respect to the laser microbeam. We also noticed a nonsymmetric laser-induced lesion in the preceding figures. This may be attributed to three things: (1) the use of a low NA (20×) objective, which is not corrected for aberrations; (2) movement of the sample during the process of laser irradiation, and (3) a defocused laser beam. Ideally, high quality phase images along with quantitative information can be obtained through the use of high NA phase objectives with a perfectly aligned, focused laser microbeam. For example, symmetric phase variations [Fig. 3(h)] were observed by use of a 40×/0.65 NA objective. Figure 3(i) shows the lesion when the laser scissors beam is slightly out of the perfect focus position in Fig. 3(h).

In Fig. 4, we show a working model of the phase change observed in laser microirradiated and collateral regions of the RBC. Figure 4(a) shows the cross-sectional view of an unirradiated RBC. Membrane damage at the microirradiated spot can cause an opening of the membrane, leading to a decrease in phase at the center of the irradiated spot. The associated buckling at collateral positions [Fig. 4(b)] leads to an increase in phase. With an increase in laser dose, an increase in membrane damage along the axial direction occurs, implying a larger decrease in phase [Fig. 4(c)]. In the case of very small laser microbeam exposures and for fresh RBCs (or other cell membranes) in a suitable buffer, it is possible to observe the resealing of the membrane after switching off the laser microbeam [Fig. 4(d)].

In conclusion, we have demonstrated a quantitative phase laser microsurgery system, which takes advantage of the combination of laser scissors and short-coherence interference microscopy. Quantitative phase images recorded during the process of laser microsurgery of red blood cells allowed evaluation of dynamic changes in phase in real time. The introduction of quantitative phase imaging in laser microscopy systems would enable quantitative evaluation of the dynamics of damage and/or repair of the cellular structures (such as chromosomes, cell membranes, and neuronal axons) subsequent to laser injury.

Acknowledgments

This work is supported by the National Institutes of Health (EB-00293, CA-91717, and RR-01192) and the Air Force Office of Science Research (FA9550-04-1-0101 and F9620-00-1-0371). Support from the Beckman Laser Institute Inc. Foundation is also gratefully acknowledged.

References

1. M. W. Berns, "*In vitro* production of chromosomal lesions with an argon laser microbeam," *Nature (London)* **221**, 74– (1969).
2. M. W. Berns, "Laser micro-surgery in cell and developmental biology," *Science* **213**, 505–513 (1981).
3. W. Tao, J. Wilkinson, E. J. Stanbridge, and M. W. Berns, "Direct gene-transfer into human cultured-cells facilitated by laser micropuncture of the cell-membrane," *Proc. Natl. Acad. Sci. U.S.A.* **84**, 4180–4184 (1987).
4. S. K. Mohanty, M. Sharma, and P. K. Gupta, "Laser-assisted microinjection into targeted animal cells," *Biotechnol. Lett.* **25**, 895–899 (2003).
5. C. E. Sims, G. D. Meredith, T. B. Krasieva, M. W. Berns, B. J. Tromberg, and N. L. Allbritton, "Laser-micropipet combination for single-cell analysis," *Anal. Chem.* **70**, 4570–4577 (1998).
6. M. Chalfie, J. E. Sulston, J. G. White, E. Southgate, J. N. Thomson, and S. Brenner, "The neural circuit for touch sensitivity in Caenorhabditis elegans," *J. Neurosci.* **5**, 956–964 (1985).
7. Y. Tadir, J. Neev, and M. W. Berns, "Laser in assisted reproduction and genetics," *J. Assist Reprod. Genet.* **9**, 303–305 (1992).
8. K. F. A. Ross, *Phase Contrast and Interference Microscopy for Cell Biologists*, Edward Arnold Publishers, London (1967).
9. R. D. Allen, G. B. David, and G. Nomarski, "The Zeiss-Nomarski differential equipment for transmitted light microscopy," *Z. Wiss. Mickrosk.* **69**, 193–221 (1969).
10. A. Barty, K. A. Nugent, D. Paganin, and A. Roberts, "Quantitative optical phase microscopy," *Opt. Lett.* **23**, 817–819 (1998).
11. E. Cuche, F. Bevilacqua, and C. Depeursinge, "Digital holography for quantitative phase-contrast imaging," *Opt. Lett.* **24**, 291–293 (1999).
12. G. Popescu, L. P. Deflores, J. C. Vaughan, K. Badizadegan, H. Iwai, R. R. Dasari, and M. S. Feld, "Fourier phase microscopy for investigation of biological structures and dynamics," *Opt. Lett.* **29**, 2503–2505 (2004).
13. C. G. Rylander, D. P. Dave, T. Akkin, T. E. Milner, K. R. Diller, and A. J. Welch, "Quantitative phase-contrast imaging of cells with phase-sensitive optical coherence microscopy," *Opt. Lett.* **29**, 1509–1511 (2004).
14. C. J. Mann, L. F. Yu, C. M. Lo, and M. K. Kim, "High-resolution quantitative phase-contrast microscopy by digital holography," *Opt. Express* **13**, 8693–8698 (2005).
15. C. J. R. Sheppard, and M. Roy, "Low-coherence interference microscopy," in *Optical Imaging and Microscopy*, P. Török and F.-J. Kao, Eds., pp. 257–274 Springer, Berlin (2003).
16. M. Hammer, D. Schweitzer, B. Michel, E. Thamm, and A. Kolb, "Single scattering by red blood cells," *Appl. Opt.* **37**, 7410–7418 (1998).
17. A. Dunn and R. Richards-Kortum, "Three-dimensional computation of light scattering from cells," *IEEE J. Sel. Top. Quantum Electron.* **2**, 898–905 (1996).